A role for regulated binding of p150^{Glued} to microtubule plus ends in organelle transport

Patricia S. Vaughan, Pedro Miura, Matthew Henderson, Belinda Byrne, and Kevin T. Vaughan

Department of Biological Sciences, University of Notre Dame, Notre Dame, IN 46556

A subset of microtubule-associated proteins, including cytoplasmic linker protein (CLIP)-170, dynactin, EB1, adenomatous polyposis coli, cytoplasmic dynein, CLASPs, and LIS-1, has been shown recently to target to the plus ends of microtubules. The mechanisms and functions of this binding specificity are not understood, although a role in encouraging microtubule elongation has been proposed. To extend previous work on the role of dynactin in organelle transport, we analyzed p150^{Glued} by live-cell imaging. Time-lapse analysis of p150^{Glued} revealed targeting to the plus ends of growing microtubules, requiring the NH$_2$-terminal cytoskeleton-associated protein–glycine rich domain, but not EB1 or CLIP-170. Effectors of protein kinase A modulated microtubule binding and suggested p150^{Glued} phosphorylation as a factor in plus-end binding specificity. Using a phosphosensitive monoclonal antibody, we mapped the site of p150^{Glued} phosphorylation to Ser-19. In vivo and in vitro analysis of phosphorylation site mutants revealed that p150^{Glued} phosphorylation mediates dynamic binding to microtubules. To address the function of dynamic binding, we imaged GFP-p150^{Glued} during the dynein-dependent transport of Golgi membranes. Live-cell analysis revealed a transient interaction between Golgi membranes and GFP-p150^{Glued}–labeled microtubules just prior to transport, implicating microtubules and dynactin in a search–capture mechanism for minus-end–directed organelles.

Introduction

Microtubule motor proteins play an important role in the translocation of many cargos, including organelles, chromosomes, and axonal components. During mitosis, these motors also contribute to spindle organization, elongation, and positioning. Among the outstanding questions is how these motors interact with cargo. For cytoplasmic dynein, several lines of evidence implicate the dynactin complex as a mediator of cargo binding. Dynactin is a large multisubunit complex first identified as a cytoplasmic dynein accessory factor which could stimulate the frequency of dynein-dependent vesicle movements in vitro (Gill et al., 1991; Schroer and Sheetz, 1991). Subsequent protein–protein interaction assays have identified the p150^{Glued} subunit of dynactin as a specific binding partner for the intermediate chains (ICs)* of cytoplasmic

dynein, implicating dynactin as an adaptor or receptor for cytoplasmic dynein on cargo (Karki and Holzbaur, 1995; Vaughan and Vallee, 1995).

To evaluate a role for dynactin as a cytoplasmic dynein receptor, we determined the distribution of dynactin in cultured cells and identified a novel population of dynactin which localized to the plus ends of microtubules and colocalized with cytoplasmic dynein (Vaughan et al., 1999; Habermann et al., 2001). Interest in this novel microtubule plus-end–associated population of dynactin was fueled further by the detection of additional proteins at these sites, including: cytoplasmic linker protein (CLIP)-170 (Pierre et al., 1992; Dujardin et al., 1998; Perez et al., 1999; Valetti et al., 1999; Vaughan et al., 1999); adenomatous polyposis coli (APC) (Nathke et al., 1996; Mimori-Kiyosue et al., 2000a); EB1 (Morrison et al., 1998; Faulkner et al., 2000; Mimori-Kiyosue et al., 2000b); CLIP-115 (Hoogenraad et al., 2000); CLASPs (Akhmanova et al., 2001); and LIS-1 (Faulkner et al., 2000; Coquelle et al., 2002). CLIP-170 has been proposed to attract dynactin to plus ends (Dujardin et al., 1998; Valetti et al., 1999; Coquelle et al., 2002). EB1 can associate with dynactin in vitro (Berrueta et al., 1999), colocalizes with dynactin at microtubule ends (Faulkner et al., 2000), and might also be involved in dynactin targeting. Cytoplasmic dynein also interacts with LIS-1 (Tai et al., 2002), and LIS-1 overexpression displaces dynactin but not EB1 from micro-

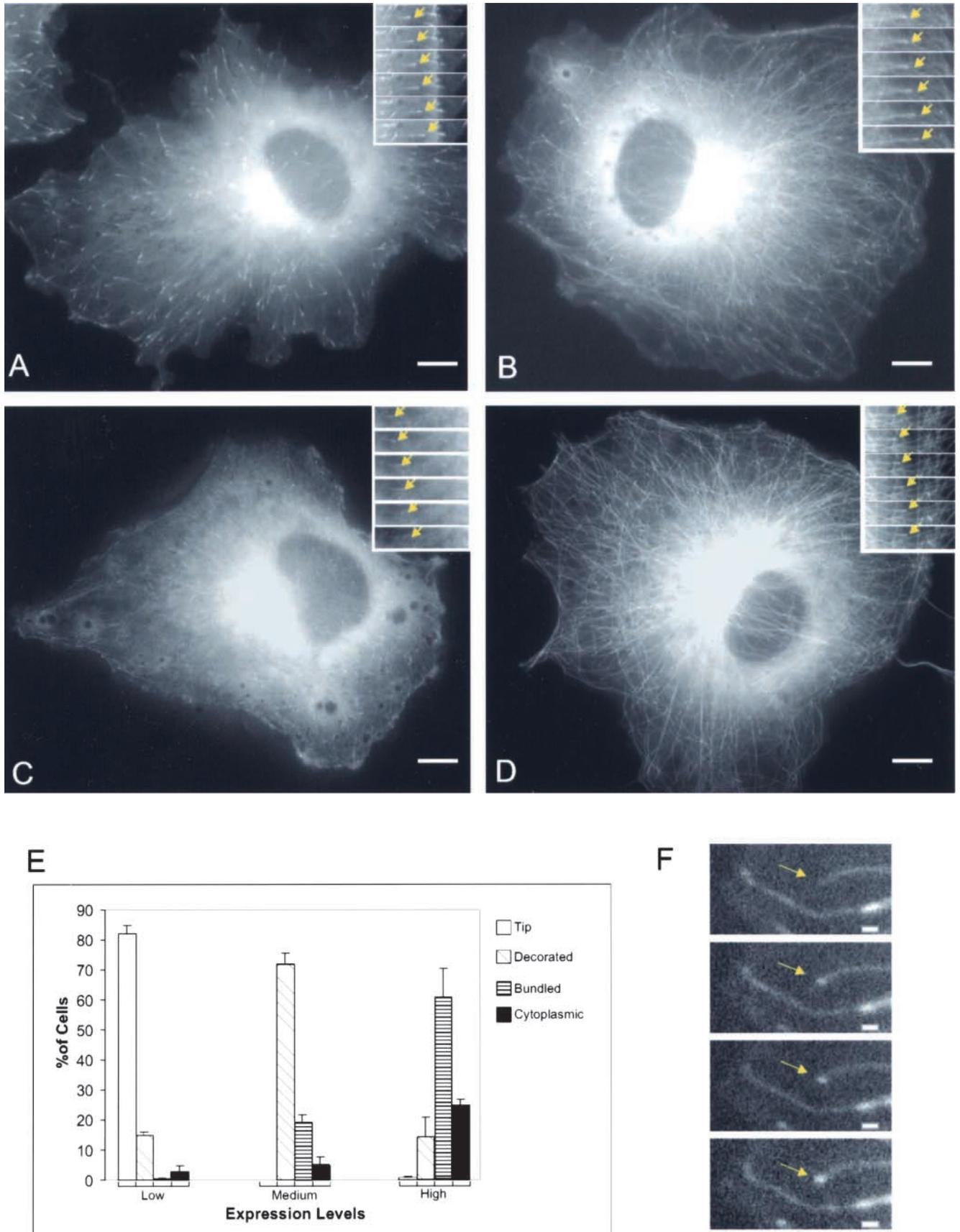Figure 1.   **p150^{Glued} binds dynamically to elongating microtubules.** (A–D) COS-7 cells transfected with expression constructs encoding GFP fusions with full-length p150^{Glued} (A, C, and D) or truncated p150^{Glued} $_{1-330}$ (B) were analyzed by live-cell imaging. Stills from time-lapse series are presented and Quick-Time movies are available at http://www.jcb.org/cgi/content/full/jcb.200201029/DC1. Time lapse images were

Table I. **Morphometric analysis of dynamic p150^{Glued} microtubule binding**

Construct	Rate of growth	Length of microtubule labeling
	$\mu m/s$	μm
p150^{Glued}		
Full-length	0.30 ± 0.03	1.57 ± 0.35
aa 1–330	0.23 ± 0.02	1.25 ± 0.24
Acetate	0.19 ± 0.04	1.06 ± 0.20
Temperature shift	0.15 ± 0.02	ND

Image stacks were imported into Metamorph for calibrated measurement of dynactin labeling and rates of microtubule growth.

tubule ends (Faulkner et al., 2000). Additional evidence for a functional link comes from analysis in genetic organisms such as *Aspergillus*, where *nudA* (cytoplasmic dynein) targets to growing microtubules tips in a dynactin-dependent manner (Xiang et al., 2000).

This complexity of proteins at microtubule plus ends suggests an important function. To determine the molecular basis of dynactin targeting, we have expressed GFP-p150^{Glued} fusions in cultured cells. Live-cell imaging of GFP-p150^{Glued} reveals a dynamic and regulated interaction of dynactin with growing microtubule plus ends. We have mapped the site of p150^{Glued} phosphorylation and tested the impact of phosphorylation on microtubule binding. Finally, imaging of p150^{Glued} with minus-end–directed organelles suggests that this dynamic association with microtubules is an important factor in the initial stages of membrane transport.

Results

Targeting of p150^{Glued} to elongating microtubules

Although antibodies to the dynactin subunits p150^{Glued}, Arp1, p50(dynamitin), and p62 have each been shown to label a population of dynactin associated with microtubule plus ends (Garces et al., 1999; Valetti et al., 1999; Vaughan et al., 1999), some antibodies to p150^{Glued} have not revealed a specific association with plus ends (Paschal et al., 1993; Waterman-Storer et al., 1995), and p150^{Glued} (Waterman-Storer et al., 1995), Arp1 (Holleran et al., 1996), and p62 (Garces et al., 1999) were not specific for plus ends when overexpressed. To minimize limitations of fixation and staining, we generated a GFP fusion to the NH$_2$ terminus of full-length p150^{Glued} and performed live-cell imaging on transfectants. We observed a wide range of expression levels which were binned into four groups based on phenotype and levels of GFP intensity (Fig. 1 E). Images collected from cells expressing GFP-p150^{Glued} at medium and high levels were consistent with previous studies in which the transfected p150^{Glued} decorated microtubules along their lengths and appeared to induce microtubule bundling (Waterman-Storer et al., 1995). Using sensitive cameras, we detected another population of cells expressing GFP-p150^{Glued} at lower levels in which the p150^{Glued} was detected at the distal ends of microtubules (Fig. 1 A). These labeled microtubule ends

were similar to the comet tail patterns observed previously for endogenous dynactin (Valetti et al., 1999; Vaughan et al., 1999) with intense labeling at the microtubule tips diminishing as a function of distance from the tips (Fig. 1 A, inset).

Previously, we recognized that dynactin bound to only a subset of microtubules; however, the molecular basis of binding specificity was elusive (Vaughan et al., 1999). Live analysis demonstrated that GFP-p150^{Glued} interacted exclusively with microtubule plus ends undergoing elongation (Fig. 1 A; Video 1, available at http://www.jcb.org/cgi/content/full/jcb.200201029/DC1). Microtubules labeled with GFP-p150^{Glued} elongated at rates (Table I) consistent with previous measurements in cultured cells (Sammak and Borisy, 1988; Dhamodharan and Wadsworth, 1995), and the number of microtubules exhibiting p150^{Glued} binding was consistent with the number observed in fixed cells previously (Vaughan et al., 1999). The length of the GFP-p150^{Glued} labeling (1.57 μm ± 0.35) was not significantly shorter than that of endogenous dynactin in fixed cells (2.22 μm ± 1.23; Vaughan et al., 1999). Segmented histogram analysis of the pixel intensities in Fig. 1 A revealed that 43.6% of the pixels reflected microtubule-associated p150^{Glued}, whereas 26.3% of the pixels reflected cytoplasmic pools not associated with microtubules (the remainder were in perinuclear region).

To define the mechanisms of targeting in greater detail, we mapped the domain of p150^{Glued} responsible for the binding to growing microtubule plus ends. Using a panel of truncation mutants, we determined that the NH$_2$-terminal 330-aa domain was sufficient for this targeting (Fig. 1 B; Video 2, available at http://www.jcb.org/cgi/content/full/jcb.200201029/DC1) and was indistinguishable from full-length p150^{Glued}. Although slightly slower (Table I), the number of microtubules labeled by the truncated GFP-p150^{Glued} fusion and the size of the comets were consistent with full-length p150^{Glued}. A construct encoding aa 1–200 also targeted to microtubule plus ends; however, this small construct also filled the nucleus (unpublished data) which complicated imaging.

Modulation of microtubule binding

Previous analysis of p150^{Glued} and dynactin in fixed cells suggested that the binding to microtubule distal ends could be

collected at 1-s intervals (insets). Transfected cells were subjected to acetate treatment (C) or temperature-shift (D). (E) The expression levels and microtubule-binding phenotypes of transfected cells were measured and used to bin cells into four catagories: tip-specific binding, microtubule decoration, microtubule binding, and soluble cytoplasmic. Cell percentages represent the average of three experiments and error bars depict standard deviation of the mean. (F) A single microtubule was visualized during the transition from shrinkage to elongation at the cell periphery. Bars: (A–D) 10 μm; (F) 1 μm.
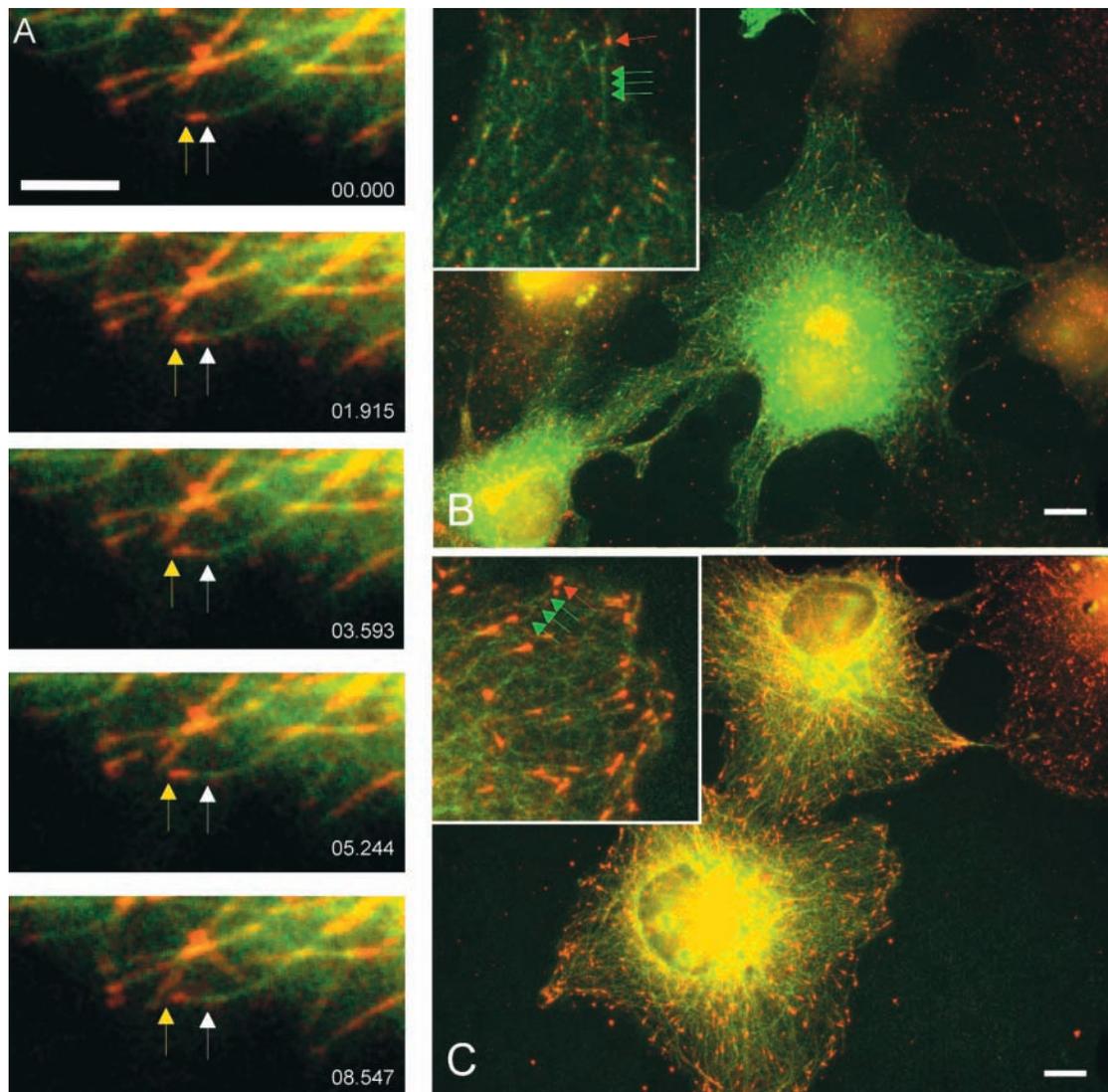
Figure 2. **Microtubule plus-end–specific binding of p150^{Glued}**. (A) Cells transfected with RFP-p150^{Glued} and GFP-tubulin were subjected to live-cell imaging and analyzed as time-lapse movies. The white arrow shows the initial position of RFP-p150^{Glued} while the yellow arrow shows the growing microtubule tip. Elapsed time of sequence is reported in lower right corner (s.ms). (B and C) Cells transfected with GFP-p150^{Glued}$_{1–330}$ (green) were fixed with methanol and labeled by IFM for CLIP-170 (B, red) or EB1 (C, red). Insets show higher magnification of GFP-p150^{Glued} (green arrows), CLIP-170 (red arrows), and EB1 (red arrows). Bars: (A) 5 μm; (B and C) 10 μm.

modulated (Vaughan et al., 1999). Acetate treatment resulted in diminished microtubule binding, a shift to lower temperature enhanced binding to the distal ends, and overexpression resulted in uniform labeling along the microtubule length (Waterman-Storer et al., 1995). To elucidate how these variables affect microtubule binding in living cells, we analyzed GFP-p150^{Glued} transfectants after acetate treatment and temperature shift. Acetate-treated cells displayed diminished binding to microtubule distal ends (Table I). Time-lapse movies revealed that acetate treatment did not inhibit the association with elongating microtubule plus ends, but did reduce the length of the comet tails (Fig. 1 C; Video 3, available at http://www.jcb.org/cgi/content/full/jcb.200201029/DC1). This reduction was coupled with a more significant soluble pool, as measured by segmented histogram analysis of pixel intensities in which 20.4% of pixels reflected microtubule-bound p150^{Glued}, and 65.7% reflected nonmicrotubule-associated p150^{Glued}.

In contrast, temperature shift of GFP-p150^{Glued}-expressing cells revealed enhanced microtubule binding. Time-lapse movies revealed that the GFP-p150^{Glued} bound microtubule distal ends but displayed more extensive comet tails (Table I). In some cases, microtubule binding was so enhanced that it resembled microtubule decoration (Fig. 1 D; Video 4, available at http://www.jcb.org/cgi/content/full/jcb.200201029/DC1). This was accompanied by a decrease in the soluble pool of GFP-p150^{Glued} as measured by segmented histogram analysis of pixel intensities in which 72% of the p150^{Glued} was microtubule associated and 6.5% was not microtubule associated.

To address whether p150^{Glued} was recruited from the cytoplasm to the microtubule during elongation or translocates towards the plus ends similar to APC (Mimori-Kiyosue et al., 2000a), we applied fluorescence speckle analysis (FSM) to our movies (Waterman-Storer et al., 1998). We did not
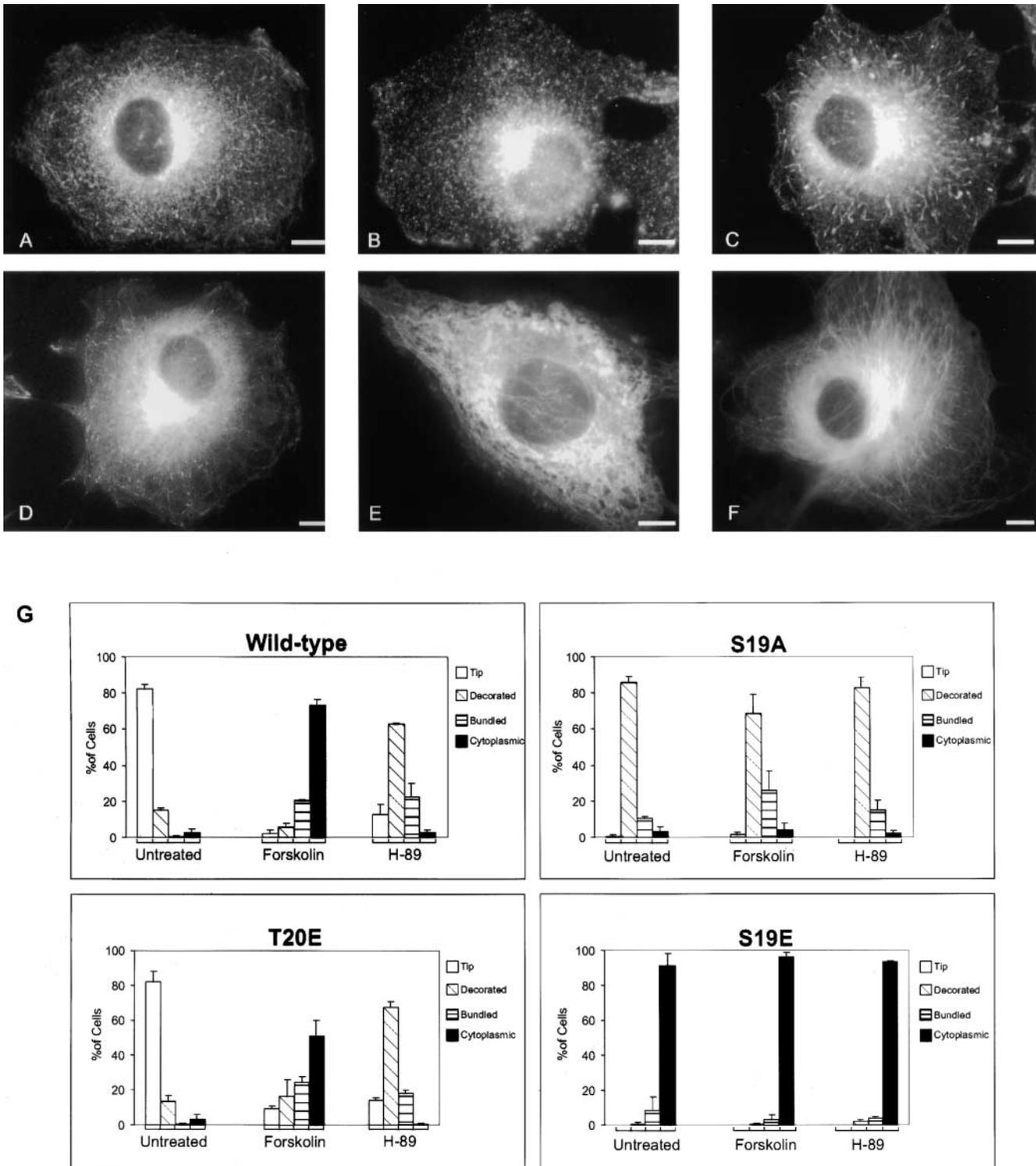
Figure 3.   **Modulation of p150^{Glued} targeting by effectors of protein kinase.** (A) COS-7 cells were either methanol fixed and stained for p150^{Glued} (A–C) or transfected with GFP-p150^{Glued} and imaged as live cells (D–F). Microtubule-binding of p150^{Glued} was compared between control cells (A and D), cells treated with 20 μM forskolin (B and E), or cells treated with 56 nM H-89 (C and F) for 2 h. Bars, 10 μm. (G) GFP fluorescence of transfected cells was measured by quantitative fluorescence microscopy and cells exhibiting low levels of expression were binned as in Fig. 1. The four panels reflect analysis of wild-type p150^{Glued}, S19A, S19E, and T20E mutants that were treated with forskolin, H-89, or left untreated. Cell percentages represent the average of three experiments and error bars depict standard deviation of the mean.
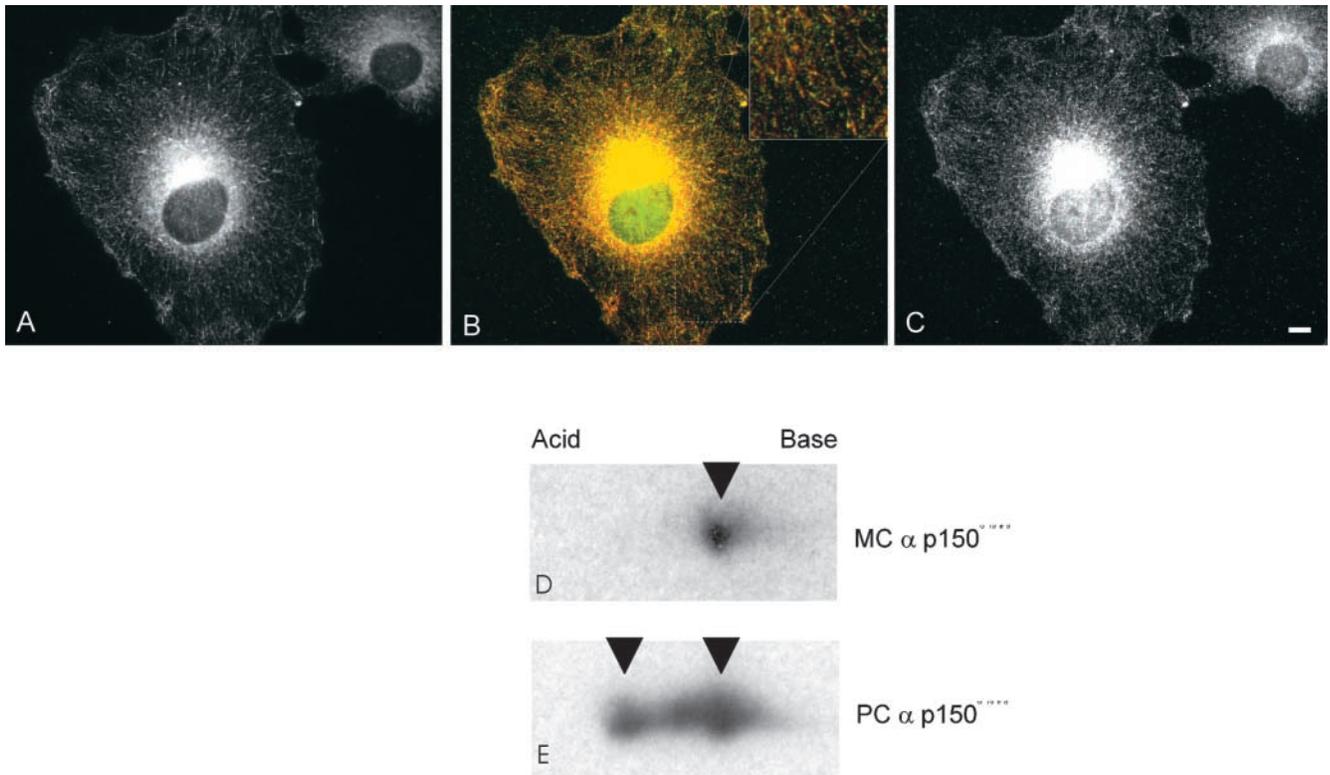
Figure 4.   **Differential binding of anti-p150^{Glued} antibodies.** COS-7 cells were methanol fixed and stained for endogenous p150^{Glued} using both monoclonal (A) and polyclonal antibodies (C). (B) Overlay of A and C highlights colocalization of both antibodies on microtubules (yellow) but not on cytoplasmic structures (polyclonal in green). Bar, 10 μm. (D and E) Two-dimensional PAGE of brain extract followed by Western blot analysis with monoclonal (D) and polyclonal (E) anti-p150^{Glued} antibodies.

detect convincing speckles by FSM, potentially due to the transient nature of p150^{Glued} binding. As an alternative, we imaged GFP-p150^{Glued} during transitions between shrinkage and growth and observed that GFP intensity increased rapidly as microtubules initiated an elongation phase (Fig. 1 F; Video 5 available at http://www.jcb.org/cgi/content/full/jcb.200201029/DC1). No comparable GFP fluorescence was observed in adjacent regions of the microtubule during this tip elongation, suggesting that the GFP-p150^{Glued} was being recruited from the cytoplasm rather than translocating towards the plus end.

Specificity of p150^{Glued} for microtubule plus ends

The precise proximity of dynactin (Valetti et al., 1999; Vaughan et al., 1999), CLIP-170 (Pierre et al., 1992), APC (Nathke et al., 1996; Mimori-Kiyosue et al., 2000a), and EB1 (Morrison et al., 1998; Mimori-Kiyosue et al., 2000b) to the microtubule plus end has been controversial. To define this parameter for p150^{Glued}, we prepared red fluorescent protein (RFP)-p150^{Glued}, cotransfected this construct with GFP-tubulin, and determined the distribution of dynamic microtubules. Similar to GFP-p150^{Glued}, RFP-p150^{Glued} targeted to microtubule distal ends and colocalized with the microtubule tip visualized via GFP-tubulin (Fig. 2 A). RFP-p150^{Glued} maintained this specificity for microtubule plus end as the microtubule elongated, suggesting that p150^{Glued} either coassembles with the elongating microtubule plus

ends, or recognizes some molecular determinant at the very tip of these microtubules.

Dynactin, EB1, and CLIP-170 bind the same microtubule ends

The specific association of GFP-p150^{Glued} with the plus ends of growing microtubules suggested binding to newly polymerized tubulin or to the GTP cap (for review see Desai and Mitchison, 1997). However, studies on CLIP-170 (Dujardin et al., 1998; Valetti et al., 1999), EB1 (Morrison et al., 1998; Berrueta et al., 1999), and LIS-1 (Faulkner et al., 2000; Coquelle et al., 2002; Tai et al., 2002) have suggested that the targeting of dynactin might require interactions with other microtubule binding proteins. To test this possibility, we analyzed the distributions of CLIP-170 and EB1 in cells expressing GFP-p150^{Glued} (Fig. 2, B and C). One striking difference between the GFP-p150^{Glued} and CLIP-170/EB1 was that the GFP-p150^{Glued} exhibited continuous fine labeling on the microtubule, whereas antibody staining for endogenous CLIP-170 and EB1 was coarse and discontinuous. Although both CLIP-170 (Fig. 2 B) and EB1 (Fig. 2 C) were targeted to the same microtubules as GFP-p150^{Glued}, neither colocalized precisely with GFP-p150^{Glued}, and in most cases, the GFP-p150^{Glued} extended further along the microtubule end than either CLIP-170 or EB1. In addition, GFP-p150^{Glued} labeled the length of microtubules when

Figure 5. **Mapping of phosphosensitive antibody epitope.** (A) Western blot analysis of bacterially expressed recombinant p150*Glued* fragments containing aa 1–811 and 39–1280 (I, bacterial culture induced with IPTG; U, uninduced) probed with polyclonal (left) and monoclonal (right) anti-p150*Glued* antibodies (B) aa 1–38 contains four consensus PKA sites (R-X$_{1,2}$-S/T), and the region of highest antigenic index predicted by the Jameson-Wolf algorithm. (C) Total cell lysates of COS-7 cells expressing wild-type p150*Glued* and site-directed mutants at S14, S19, and T20 were probed by Western blot analysis using monoclonal (top) and polyclonal (bottom) anti-p150*Glued* antibodies. (D) Wild-type and S19A polypeptides were phosphorylated in vitro by PKA for the indicated times (min). Phosphorylated samples were subjected to Western blot analysis with first monoclonal and then polyclonal anti-p150*Glued* antibodies.

expressed at high levels, labeling regions of microtubules where neither CLIP-170 nor EB1 was detected (unpublished data). This suggests that p150*Glued* can bind microtubules independently of CLIP-170 and EB1.

Protein kinase effectors alter p150*Glued* binding
Because phosphorylation has been implicated in regulating the microtubule-binding properties of CLIP-170 (Rickard and Kreis, 1991) and p150*Glued* (Farshori and Holzbaur, 1997; Reese and Haimo, 2000), we screened a panel of kinase activators and inhibitors for effects on the targeting of p150*Glued* to microtubule plus ends. As an assay, we used immunofluorescence microscopy (IFM) analysis of endogenous dynactin which reveals both randomized and microtubule-bound populations of punctate staining (Fig. 3 A) (Valetti et al., 1999; Vaughan et al., 1999). Stimulation

of protein kinase A (PKA) through forskolin treatment changed the pattern of dynactin significantly, eliminating the microtubule-associated population (Fig. 3 B). This was accompanied by a more pronounced randomized population of dynactin puncta. In contrast, H-89, which inhibits PKA (Fig. 3 C) enhanced the binding of dynactin to microtubules. This was coupled with a decrease in the randomized population of dynactin.

To test the specificity of these effects for the p150^{Glued} subunit of dynactin, we treated cells expressing GFP-p150^{Glued} as above and monitored microtubule binding in living cells. Forskolin treatment diminished microtubule binding (Fig. 3, E and G), whereas H-89 treatment enhanced microtubule binding dramatically (Fig. 3, F and G) when compared with untreated cells (Fig. 3 D). As indicated above (Fig. 1, C and D), segmented histogram analysis revealed that decreased microtubule binding correlated with an increased soluble pool, whereas enhanced microtubule binding correlated with a lower soluble pool. Because forskolin stimulates kinase activity and H-89 inhibits kinase activity, these findings suggest that p150^{Glued} phosphorylation releases p150^{Glued} from microtubules and that this phosphorylation is an important component of plus-end–specific binding.

Identification of a p150^{Glued} phosphorylation site

Another indication of p150^{Glued} phosphorylation stemmed from analysis of dynactin in fixed cells using two antibodies to p150^{Glued} (Fig. 4). When these two antibodies were used to localize dynactin, we observed an intriguing difference in labeling. Both antibodies were generated against the NH$_2$-terminal 200 aa of rat brain p150^{Glued}; however, the monoclonal antibody labeled only a subset of the p150^{Glued} detected by the polyclonal antibody (Vaughan et al., 1999). Whereas the polyclonal antibody detected both the microtubule-associated population and the randomized population (Fig. 4, B and C), the monoclonal detected primarily the microtubule-associated fraction (Fig. 4, A and B). COS-7 cells express only one p150^{Glued} polypeptide (Vaughan et al., 1999), implicating a posttranslational modification as the basis of differential binding.

To test this possibility, we performed two-dimensional gel Western blot analysis using the two antibodies to p150^{Glued}. The polyclonal antibody detected multiple isoelectric variants in these samples, suggesting phosphorylation of a single polypeptide (Fig. 4 D). In contrast, the monoclonal antibody detected only the most basic isoelectric variant, predicted to be the dephosphorylated form of the protein (Fig. 4 E).

The cell localization studies and two-dimensional gel analysis suggested that the monoclonal antibody was sensitive to p150^{Glued} phosphorylation. To test this hypothesis, we mapped the epitope of the monoclonal antibody which was predicted to encompass a p150^{Glued} phosphorylation site. We performed Western blot analysis on a panel of p150^{Glued} truncation mutants and compared the binding of polyclonal and monoclonal antibodies (Fig. 5 A). Whereas the polyclonal antibody detected both mutants, the monoclonal antibody detected the aa 1–811 construct, but not the aa 39–1280 construct. This result focused our attention on the NH$_2$-terminal 38 aa of 150^{Glued} which lies just upstream of

the predicted microtubule binding domain of p150^{Glued} and contains the highest antigenic index of the protein as predicted by the Jameson-Wolf algorithm (Fig. 5 B).

Our analysis of drugs which affect the activity of PKA suggested that the p150^{Glued} phosphorylation site and the monoclonal antibody epitope would match the consensus for PKA (R/K-X$_{1,2}$-S/T). Within the NH$_2$-terminal 38 aa of p150^{Glued}, we detected four consensus PKA sites. To test if phosphorylation at any of these sites inhibited binding of the monoclonal antibody, we systematically prepared site-directed mutations at each consensus PKA site to mimic a phosphorylated (S/T to E) or a dephosphorylated (S/T to A) form. Each of these mutants was transfected into COS-7 cells and cell lysates were separated by SDS-PAGE. Western blot analysis showed that the polyclonal antibody detected wild-type and all mutant polypeptides, whereas the monoclonal antibody detected all variants except the S19E polypeptide (Fig. 5 C). To confirm p150^{Glued} phosphorylation as the basis of diminished monoclonal antibody binding, we performed in vitro PKA phosphorylation reactions on wild-type and S19A polypeptides (Fig. 5 D). Phosphorylation was observed in both reactions, consistent with the number of consensus PKA sites in the 330 aa fragments ($n = 9$). For the wild-type protein, binding of the monoclonal decreased as phosphorylation increased, suggesting phospho-sensitive binding. In contrast, phosphorylation of the S19A mutant had no impact on monoclonal antibody binding indicating specific sensitivity to phosphorylation at S19.

p150^{Glued} phosphorylation regulates microtubule binding

To correlate p150^{Glued} phosphorylation state with microtubule binding, we transfected each mutant and examined the GFP fusion proteins by live-cell imaging. Mutations at S14 and T20 had no impact on dynamic microtubule binding (Fig. 6 A, S14A and T20E). These constructs were indistinguishable from the wild-type aa 1–330 polypeptide, with specificity to microtubule plus ends at low levels of expression (Fig. 3 G), and more extensive microtubule labeling at high levels of expression (unpublished data). In contrast, mutations to S19 had a dramatic effect on microtubule binding (Figs. 3 G and 6 A, S19A and S19E). The S19A mutant bound microtubules along their lengths, even at low levels of expression (Figs. 3 G and 6 A). However, the S19E mutant did not display significant binding to microtubules in these live-cell assays (Figs. 3 G and 6 A). The S19E mutant was primarily soluble even at low levels of expression where microtubule binding would be most obvious (Fig. 3 G).

To determine if p150^{Glued} phosphorylation regulated microtubule binding directly, we prepared recombinant wild-type and mutant p150^{Glued} polypeptides and tested their ability to bind tubulin in an overlay assay (Fig. 6 B). Similar to previous work (Vaughan and Vallee, 1995), we observed binding of wild-type p150^{Glued} and both S19A and T20E mutants to tubulin, consistent with the results in living cells. However, analysis of the S19E mutant revealed diminished tubulin binding. Although the difference in binding was substantial within the linear range of detection, longer exposures revealed a low level of tubulin binding for the S19E
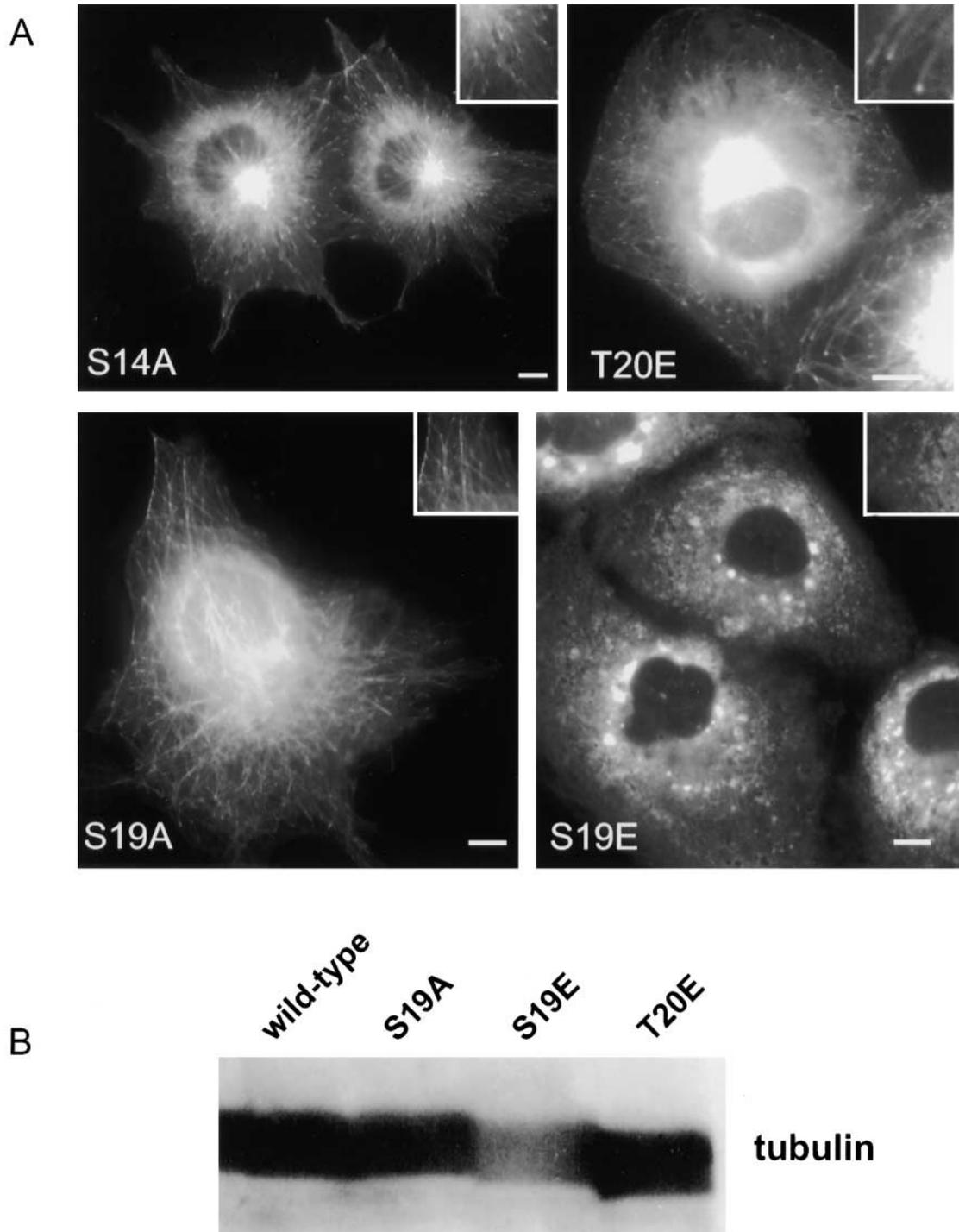
Figure 6. **Site-directed mutagenesis of candidate p150^{Glued} phosphorylation sites.** (A) GFP-p150^{Glued} $_{1–330}$ mutant constructs S14A, T20E, S19A were transfected into COS-7 cells and analyzed by live-cell imaging. Insets show higher magnification of microtubule plus ends. Bars, 10 μm. (B) Blot overlay assays comparing the binding of recombinant p150^{Glued}$_{1–330}$ and mutants to parallel strips of brain tubulin.

mutant. This is consistent with previous analysis of mutants designed to mimic a constitutively phosphorylated form of the cytoplasmic dynein ICs which displayed a 5-fold lower affinity for p150^{Glued} in vitro (Vaughan et al., 2001). The difference in binding between the S19A and S19E mutants is most consistent with regulation of microtubule binding by p150^{Glued} phosphorylation (Fig. 7).

Sensitivity of p150^{Glued} mutants to kinase effectors

Forskolin and H-89 treatment both modulated the microtubule binding activity of the wild-type p150^{Glued} polypeptide (Fig. 3), consistent with regulation of microtubule binding by p150^{Glued} phosphorylation. To confirm the identification of S19 as the p150^{Glued} phosphorylation site in vivo, we measured the ability of forskolin and H-89 to modulate the microtubule

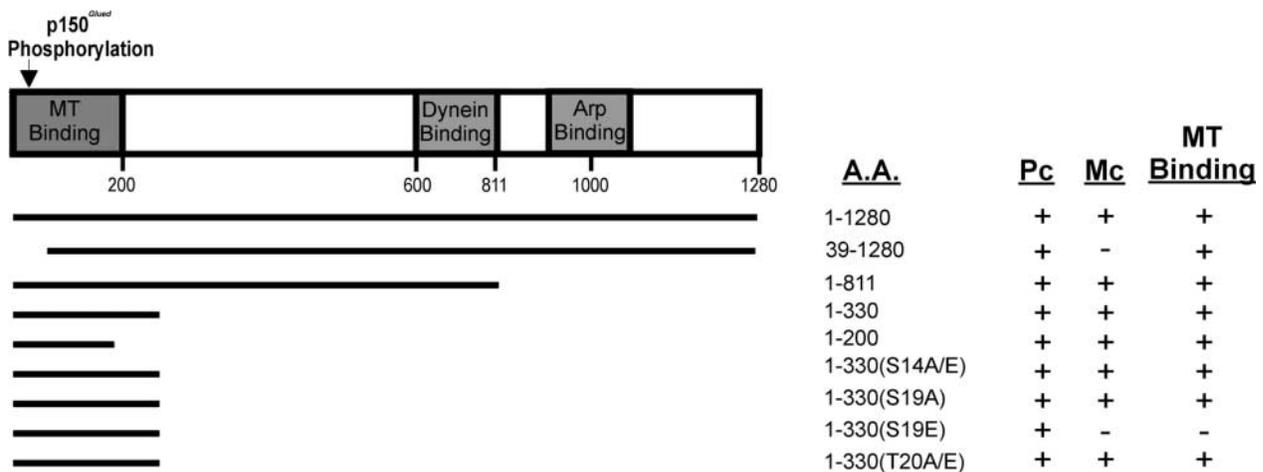| A.A.	Pc	Mc	MT Binding
1-1280	+	+	+
39-1280	+	-	+
1-811	+	+	+
1-330	+	+	+
1-200	+	+	+
1-330(S14A/E)	+	+	+
1-330(S19A)	+	+	+
1-330(S19E)	+	-	-
1-330(T20A/E)	+	+	+

Figure 7. **Summary of mutation analysis.** Line diagram depicting the positions of truncation and site-directed mutants as well as binding activities of antibodies and the microtubule-binding activity of p150^{Glued}.

binding activity of the site-directed mutants. Similar to the wild-type protein, S14 (unpublished data) and T20 mutants reacted to these drug treatments by shifting either towards the soluble state (forskolin) or microtubule-bound state (H-89) (Fig. 3 G). In contrast, the S19 mutants failed to respond to either drug treatment displaying either reduced (S19E) or enhanced (S19A) microtubule binding in both forskolin and H-89. This suggests that wild-type p150^{Glued} and S14 and T20 mutants are each substrates for phosphorylation, whereas the S19 mutants are no longer recognized by the p150^{Glued} kinase pathway.

Interactions between microtubule plus ends and minus-end–directed membranes prior to motility

To explore the potential relationship between microtubule-associated dynactin and organelle transport, we performed live-cell imaging on Golgi-derived membranes which require both dynein and dynactin for centripetal transport (Corthesy-Theulaz et al., 1992; Burkhardt et al., 1997; Presley et al., 1997). We cotransfected a construct encoding RFP–n-acetyl glucosamine transferase (NAGT) which functioned as a live-cell marker for Golgi-derived membranes (Shima et al., 1997; Vaughan et al., 2001) along with GFP-p150^{Glued}. To increase the frequency of minus-end–directed movements, we performed brefeldin A (BFA) treatment which drove the Golgi complex back into the endoplasmic reticulum (Lippincott-Schwartz et al., 1990). BFA washout was then used to synchronize a centripetal wave of membrane transport as the Golgi complex reformed. This allowed visualization of GFP-p150^{Glued} together with Golgi membranes undergoing motility (Fig. 8 A; Video 6, available at www.jcb.org/cgi/content/full/jcb.200201029/DC1). We focused on cells in which Golgi membranes were in the process of reforming ($n = 52$) and compared the position of the GFP-p150^{Glued}-positive microtubule plus ends with Golgi membranes which underwent motility during the time-lapse sequences (Fig. 8 A). In 90% ($n = 47/52$) of cells, at least one membrane underwent transport and these membranes displayed the same series of events (Fig. 8 B, insets). First, the Golgi membranes displayed apparent Brownian movement in the cytoplasm which was nonlinear and led to

no productive translocation. Next, these membranes were encountered by a GFP-p150^{Glued}-positive microtubule tip which arrested the Brownian movement and immobilized the membrane. After a brief delay (1 to 2 s), these membranes displayed rapid minus-end–directed translocation to the reforming Golgi complex at rates of 1.25 μm/s (Fig. 8 B; Video 7, available at www.jcb.org/cgi/content/full/jcb.200201029/DC1). The microtubule membrane encounters appeared stochastic; however, an interaction appeared to be a prerequisite for motility. These observations suggest that microtubules initiate contact with dynein-dependent organelles through a mechanism analogous to the search–capture model of kinetochore–microtubule interactions.

To test whether the regulated interaction of p150^{Glued} with microtubules was important for these events, we followed GFP-p150^{Glued} and RFP-tagged Golgi membranes during BFA washout in the presence of forskolin (Fig. 8 C; Video 8, available at www.jcb.org/cgi/content/full/jcb.200201029/DC1). Because forskolin diminished the binding of p150^{Glued} and dynactin to microtubules, one might predict reduced microtubule capture by the Golgi membranes. Live-cell imaging of the Golgi membranes in the presence of forskolin revealed a lack of minus-end–directed motility which inhibited Golgi reformation. Unlike Golgi membranes in control cells, in 80% ($n = 19/24$) of the forskolin-treated cells the Golgi membranes displayed extensive tubulation in the cell periphery. These tubulated membranes underwent plus-end– but not minus-end–directed excursions (Fig. 8 C, insets). These phenotypes resembled the defects during expression of dominant inhibitory cytoplasmic dynein IC phosphorylation mutants (Vaughan et al., 2001), suggesting a lack of dynein-mediated transport.

Discussion

To elucidate the behavior and function of dynactin at microtubule plus ends, we have analyzed GFP-p150^{Glued} using live-cell imaging. These studies reveal that p150^{Glued} interacts dynamically with microtubules, and that this interaction is regulated by phosphorylation. Analysis of GFP-p150^{Glued} together with Golgi-derived membranes suggests that the dy-
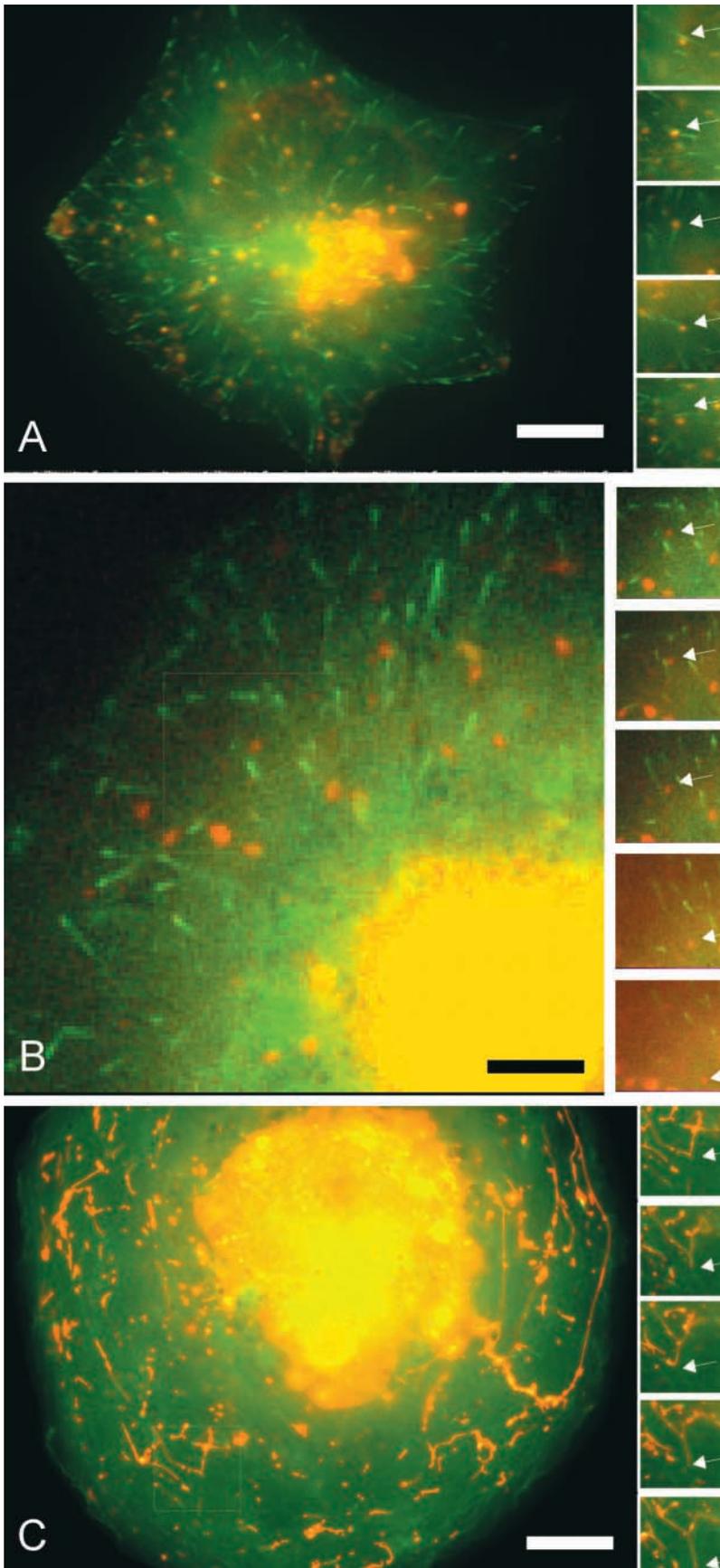
Figure 8. **Association of Golgi-derived membranes with elongating microtubule plus ends.** COS-7 cells were cotransfected with GFP-150^{Glued} (green) and RFP-tagged NAGT (red). Live-cell imaging was performed after BFA washout and sequential dual channel images were captured at ~1-s intervals. (A) One example where 15 membranes undergo minus-end–directed motility during 100 s. Each membrane interacts with a GFP-positive microtubule plus end just before motility (insets, arrows). (B) Stills from a time-lapse sequence reveal the sequence of events for one NAGT-positive membrane undergoing minus-end–directed motility (arrows). (C) Forskolin treatment during BFA washout. The inset shows that these NAGT-positive membranes display some plus-end–directed excursions (arrows), but fail to resolve into vesicles or reform with the Golgi complex. Quick-Time movies of these sequences are available at http://www.jcb.org/cgi/content/full/jcb.200201029/DC1. Bars: (A) 10 μm; (B) 4 μm; (C) 10 μm.

namic binding of dynactin to microtubule plus-ends plays a novel role in the early stages of membrane transport.

Dynamic binding of p150^{Glued} to microtubule plus-ends

Although we recognized that p150^{Glued} bound to the plus ends of microtubules, live-cell imaging revealed a specific association with growing microtubules. This conceptual advance for dynactin is intriguing because previous work links these plus ends to recruitment of cytoplasmic dynein (Vaughan et al., 1999). Analysis of truncation mutants indicates that only the NH$_2$-terminal 200 aa are required for this binding specificity, suggesting that interactions with other dynactin components (Arp1, p62) and other organelle components such as spectrin are not required for this activity.

Live-cell imaging of these GFP fusions during acetate treatment and temperature shift revealed at least two events which contribute to the comet tail appearance of these proteins; binding to the elongating microtubule plus end which is followed by a delayed release. Whereas acetate treatment and temperature shift modulated the release step, neither appeared to alter initial binding to microtubule ends. This suggests multiple molecular events at the microtubule plus end which are coordinated or occur in sequence.

Mechanisms of microtubule plus-end specificity

Among the biochemical features unique to growing microtubule plus ends is the tubulin GTP cap (for review see Desai and Mitchison, 1997). This feature could explain the unique comet tail appearance of the p150^{Glued} and dynactin. High-affinity binding to GTP-tubulin could be followed by delayed release of p150^{Glued} as GTP is hydrolyzed to GDP. Although the dimensions and variability of the GTP-cap remain controversial, the length of the GFP-p150^{Glued} comets would suggest a substantial cap of GTP-tubulin or a delay between GTP hydrolysis and p150^{Glued} release. Although this mechanism has many appealing features, several observations argue against this model. First, in cells expressing p150^{Glued} at higher levels, we and others observe that p150^{Glued} binds along the length of microtubules. The vast majority of the p150^{Glued} is bound to tubulin which is predicted to be in the GDP-state. This would argue against p150^{Glued} having specific affinity for GTP-tubulin. Second, overlay assays with recombinant p150^{Glued} and SDS-PAGE separated tubulin reveals binding in the absence of any nucleotide, undermining an important role for GTP-tubulin in plus-end binding.

A related explanation could be the unique structure at the plus end of a growing microtubule, which would change as the protofilaments closed to form a tube. Our studies do not provide sufficient resolution to address this possibility. However, the fact that p150^{Glued} can decorate microtubules at high levels of expression does not support this mechanism.

Another possibility is that p150^{Glued} interacts with another microtubule binding protein at the plus-end such as CLIP-170 or EB1 (see above). We observe binding of p150^{Glued} to microtubules in places lacking both CLIP-170 and EB1 (Fig. 2). This could implicate other proteins such as LIS-1, CLASPs, and XMAP-215 in the recruitment of p150^{Glued}. However, in vitro binding assays do not support this model

because purified recombinant p150^{Glued} binds tubulin directly in the absence of these proteins (Fig. 6 B).

Alternatively, the release step rather than the binding step could confer plus-end specificity. For example, ubiquitous binding to microtubules which is followed by slightly delayed release could also lead to plus-end–specific labeling because only newly polymerized microtubules would reveal the lag between binding and release. Analysis of microtubule release would clarify this potential explanation for plus end specificity (see below).

Regulation of microtubule binding by p150^{Glued} phosphorylation

Several lines of evidence implicate p150^{Glued} phosphorylation as a mechanism to regulate microtubule binding. Drugs that stimulate protein kinase A reduce the binding of native dynactin and GFP-p150^{Glued} to microtubules. In contrast, drugs that inhibit protein kinase A induce enhanced microtubule binding, similar to microtubule decoration. This duality of phenotypes resembles the outcome of acetate and temperature shift experiments, suggesting a similar mechanism. Furthermore, S19A and S19E mutants recapitulate these phenotypes in vitro and in vivo. Together these results suggest that the interaction between p150^{Glued} and microtubules is regulated by phosphorylation at S19.

Further support for this method of regulation was provided by earlier work with CLIP-170 (Rickard and Kreis, 1991). Similar to p150^{Glued}, CLIP-170 binds to microtubule plus-ends (Pierre et al., 1992; Valetti et al., 1999; Vaughan et al., 1999) and binds to elongating microtubule ends in live-cell imaging (Perez et al., 1999). In microtubule binding assays, CLIP-170 phosphorylation reduced microtubule-binding. The similarity in cytoskeleton-associated protein–glycine rich motifs shared by p150^{Glued} and CLIP-170 suggests similar mechanisms of regulation.

Reese and Haimo have also linked dynactin phosphorylation to regulation of function (Reese and Haimo, 2000). Whereas their work in *Xenopus* pigment granuoles implicates PKC, our work in COS-7 cells suggests a member of the PKA family. We analyzed site-directed mutants at S23 (consensus PKC site) and observed no effect on dynamic microtubule binding (unpublished data). Our negative results with PKC drugs and mapping of the p150^{Glued} phosphorylation site in COS-7 cells may indicate alternative mechanisms of regulation for specialized organelles.

If phosphorylation regulates microtubule binding, this would implicate p150^{Glued} phosphorylation as one mechanism for release at the plus end. This hypothesis could explain why microtubule decoration is observed at high levels of expression; high levels of substrate overwhelm the p150^{Glued} kinase allowing constitutive binding. This could also explain the substantial microtubule binding activity of dynactin in microtubule sedimentation assays where only a small fraction of tubulin is predicted to be undergoing polymerization. In the absence of the p150^{Glued} kinase, constitutive binding would be predicted.

Our data supports phosphorylation at S19 from six lines of reasoning: (a) S19 fits the consensus for PKA, consistent with drug treatments; (b) S19 lies within the epitope of the
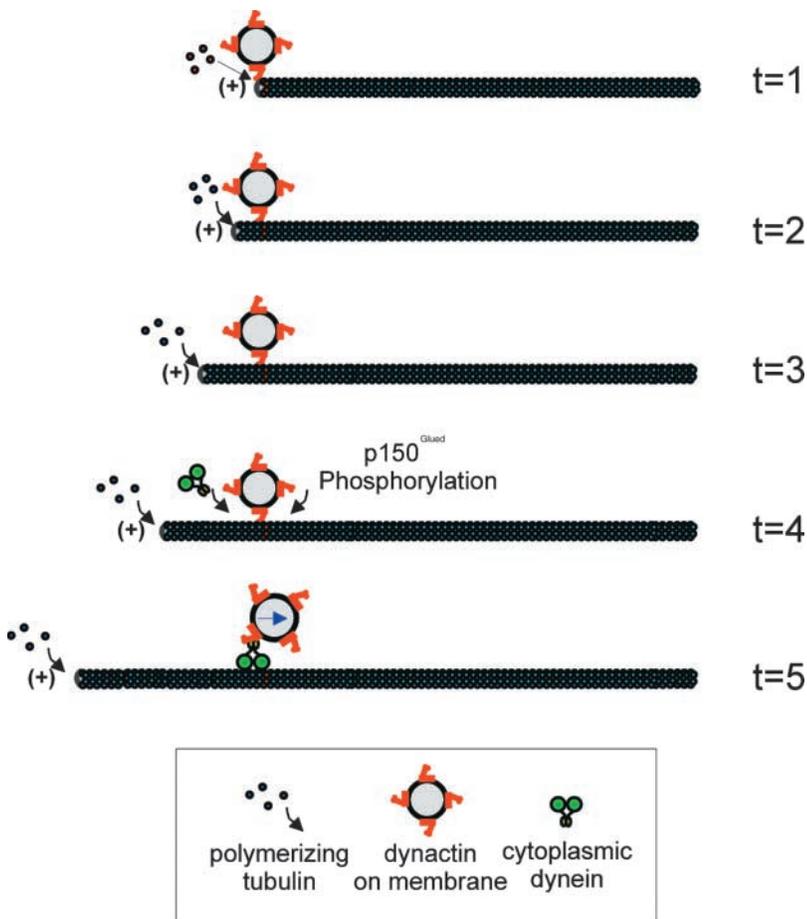
Figure 9. **Proposed role for P150^{Glued}–microtubule interactions during membrane transport.** Micro-tubule explores the cytoplasm and encounters a membrane (t = 1). Membrane-associated dynactin stabilizes the interaction and anchors the membrane while the microtubule continues to elongate (t = 2, 3). After a brief delay, the membrane-associated dynactin recruits cytoplasmic dynein (t = 4). After p150^{Glued} phosphorylation (t = 4), cytoplasmic dynein becomes the only mechanism of microtubule-association. This shift from dynactin- to dynein-mediated binding allows minus-end–directed motility of the membrane (t = 5).

phosphosensitive monoclonal antibody; (c) in vitro phosphorylation of wild-type p150^{Glued} but not the S19A mutant reduces monoclonal antibody binding; (d) S19 but not other mutants mimic the effects of PKA drugs; (e) S19 mutants also fail to respond to PKA drugs suggesting loss of the phosphorylation site; and (f) sequence alignments with other vertebrate species indicate that S19 is conserved, whereas S14 and T20 are not conserved.

Implications for minus-end–directed membrane motility

A function for specific binding to microtubule plus ends has been elusive. One could argue that binding and delayed release from microtubules provides no benefit for organelle transport. Our data suggest that dynactin functions as an opportunistic organelle component which captures microtubules as they explore the cytoplasm. Rather than membranes searching for microtubules, microtubules probe the cytoplasm for organelles to be transported. This novel mechanism would be very similar to the search-capture model proposed for kinetochore–microtubule (Mitchison and Kirschner, 1985; Huitorel and Kirschner, 1988; Hayden et al., 1990) and mitotic spindle–cortex interactions (Carminati and Stearns, 1997; Desai and Mitchison, 1997; Adames and Cooper, 2000; Schuyler and Pellman, 2001). Interestingly, many of the proteins that colocalize at microtubule plus ends also localize to kinetochores during mitosis, in-

cluding dynactin, CLIP-170, EB1, and LIS-1. This similarity in protein composition between kinetochores and organelles could suggest that both use the same mechanism to initiate interactions with microtubules. Another implication of this work is that microtubule dynamics increases the probability of membrane–microtubule interactions.

These experiments potentially provide new insight into the initial stages of minus-end–directed membrane transport in cells. The association of dynactin with the surface of membranes may play two overlapping roles in transport (Fig. 9). First, through a specific interaction of dynactin with growing microtubule plus ends, dynactin appears to stabilize a stochastic interaction between membranes and microtubules. Second, through a specific association with cytoplasmic dynein, this dynactin recruits motors for motility (Vaughan et al., 1999). These functions, together with a role in improving the processivity of cytoplasmic dynein (King and Schroer, 2000), suggest that dynactin is an important component of cytoplasmic dynein-mediated membrane transport.

Materials and methods

Expression constructs and antibodies
GFPp150$_{FL}$ was created by fusing EGFP (CLONTECH Laboratories, Inc.) to the NH$_2$ terminus of rat brain p150^{Glued} (Holzbaur et al., 1991) by PCR mutagenesis and cloned into the pCIneo expression vector (Promega) by standard cloning techniques. This construct was truncated at the AccI site at aa 330 of p150^{Glued} to create GFPp150$_{1–330}$. Mutations at S14, S19, and T20

were created by PCR site-directed mutagenesis and were inserted into the GFPp150$_{1-330}$ backbone. Bacterial expression constructs were created by inserting the wild-type and mutant p150$_{1-330}$ sequences into pET21a (Novagen). RFPp150$_{1-330}$ was created by replacing the GFP tag of GFPp150$_{1-330}$ with DsRed or DsRed2 (CLONTECH Laboratories, Inc.) by PCR mutagenesis and standard cloning techniques. Either DsRed or DsRed2 gave similar results. GFP tubulin was purchased from CLONTECH Laboratories, Inc. Truncated p150^{Glued} aa 1–811, RFP-NAGT and DPT1 (aa 39–1280) have been reported previously (Holzbaur et al., 1991; Vaughan et al., 2001). Monoclonal antibodies to p150^{Glued} and EB1 were purchased from BD Transduction Laboratories, anti–CLIP-170 was a gift of Holly Goodson (University of Notre Dame, Notre Dame, IN), and polyclonal anti-p150^{Glued} has been described previously (Vaughan et al., 1999).

Tranfections, live-cell imaging, and immunofluorescence

COS-7 cells were transfected with 1 μg total plasmid DNA and 3 μl LipofectAmine (GIBCO-BRL) as described previously (Vaughan et al., 2001), and total cell lysates were harvested 2 d after transfection. Alternatively, live-cell digital imaging was performed 1 d after transfection on a Zeiss Axiovert equipped with an Apogee KX85 cooled CCD camera run by PMIS software (GCR Consulting) as described previously (Vaughan et al., 2001). TIF image stacks were exported to Adobe Photoshop®, imported into Quick-Time to create movies, and exported as AVI files. Alternatively, dual-channel imaging was performed on cells coexpressing GFP150$_{1-330}$ and RFP-NAGT or RFP150$_{1-330}$ and GFP tubulin using Metamorph (Universal Imaging) to control a Sutter filter wheel and Coolsnap HQ digital cooled CCD camera (Roper Scientific). BFA was used at 5 μM for 2 h to redistribute the RFP-NAGT into the endoplasmic reticulum followed by 15-min washout in DME medium. For IFM, cells were methanol-fixed and stained using antibodies to CLIP-170 or EB1 and Cy3 anti–mouse secondary antibodies (Jackson ImmunoResearch Laboratories) as described previously (Vaughan et al., 1999). Acetate treatment and temperature shift experiments were performed as described previously (Vaughan et al., 1999).

Quantification of GFP-p150^{Glued} expression

All imaging was performed at the same magnification and illumination levels with 50% attenuation by neutral density filters. Accumulation levels of the GFP-p150^{Glued} fusion proteins were determined by image pixel intensity after 400 ms exposures without pixel binning. Total GFP fluorescence was quantified by integrating histogram plots of whole cells. In addition, fluorescence intensity of cytoplasmic and microtubule-associated dynactin was determined manually. Images were converted to 8-bit scale, and pixel intensities in areas identified as background, cytoplasm without microtubule labeling, microtubule-bound, and perinuclear regions were recorded using Metamorph. The values corresponding to the four levels of intensity were used to define four bins for segmented histogram analysis of each image. After thresholding and restricting analysis to the cell of interest, the percentage of pixels corresponding to each bin were recorded.

To assess the relationship between expression level and phenotype, we performed line-scan histograms on pools of 100 cells and recorded maximum pixel intensities. We binned these cells into the following groups: (a) low-level expression (within 100 units of background); (b) medium-level expression (100–800 units over background); and (c) high-level expression (everything above 800 units over background). In addition, we scored the cells as exhibiting tip-specific labeling, microtubule decoration, microtubule bundling or soluble GFP-fluorescence. Because the low-level expressors were most similar to control cells, we have presented imaging data for this population only.

Analysis of kinase effectors

Forskolin (Calbiochem) dissolved in DMSO was added to culture medium at 20 μM (inhibitory concentration [IC$_{50}$] = 10–20 μM for PKA) and cells were treated for 2 h and then fixed or imaged as living cells. In the BFA experiment, 20 μM forskolin was added to the 15-min DME washout. H-89 (Calbiochem) was dissolved in water and added to culture medium at 56 nM (IC$_{50}$ = 48 nM for PKA) for 2 h, after which cells were either fixed or imaged as living cells.

Protein expression, two-dimensional gels, Western blotting, and blot overlays

Recombinant proteins were expressed in BL21(DE3) cells, induced with 1 mM IPTG and purified as described previously (Vaughan and Vallee, 1995). For Western blots, total cell lysates from uninduced and induced cultures or transfected COS-7 cells were applied to an SDS polyacrylamide gel and transferred to Immobilon P (Millipore). For the two-dimensional

gels, the first dimension of bovine brain extracts were separated in tube gels containing 5–7 ampholytes as described previously (Vaughan et al., 2001). Second-dimension polyacrylamide gels were then transferred to Immobilon P. All blots were first probed with monoclonal anti-p150^{Glued} antibody. The same blot was then probed with polyclonal anti-p150^{Glued} antibody. P150^{Glued}-tubulin blot overlays were performed with bovine brain extract applied to an SDS-polyacrylamide gel in a curtain well and blotted to Immobilon P. Parallel strips of the blot were treated with 750 ng/ml of each overlay protein followed by polyclonal anti-p150^{Glued} antibody as described previously (Vaughan and Vallee, 1995).

PKA assays

0.5 μg of recombinant wild-type or S19A p150$_{1-330}$ were treated at 30°C for the indicated times in a 20 μl reaction with 2,500 units PKA (New England Biolabs) in supplied buffer plus 250 μM ATP and 5 μCi γ [^{32}P]ATP. Parallel samples without [^{32}P] were processed for Western blotting.

Online supplemental material

Still images presented in Figs. 1, A–D and F were derived from time-lapse image sequences which can be viewed as Quick-Time at available at http://www.jcb.org/cgi/content/full/jcb.200201029/DC1. These movies depict the behavior of GFP-p150^{Glued} fusion proteins in living cells after transfection. Videos 1 and 3–5 represent full-length p150^{Glued} under control conditions (1 and 5), acetate treatment (3) or temperature-shift (4). Video 2 depicts a truncated fusion protein containing aa 1–330 of p150^{Glued}.

Quick-Time movies of Fig. 8 (A–C) depict time-lapse sequences of cells transfected with GFP-p150^{Glued} and RFP-tagged NAGT. Video 6 documents a cell in which most of the organelles undergo centripetal movement during the time-lapse sequence. Each membrane interacts with a GFP-p150^{Glued} labeling microtubule plus end just prior to motility. Video 7 represents an example where the specific steps in the loading process are revealed. Video 8 documents the effects of forskolin on Golgi reformation.

References

Adames, N.R., and J.A. Cooper. 2000. Microtubule interactions with the cell cortex causing nuclear movements in *Saccharomyces cerevisiae*. *J. Cell Biol.* 149: 863–874.

Akhmanova, A., C.C. Hoogenraad, K. Drabek, T. Stepanova, B. Dortland, T. Verkerk, W. Vermeulen, B.M. Burgering, C.I. De Zeeuw, F. Grosveld, and N. Galjart. 2001. Clasps are CLIP-115 and -170 associating proteins involved in the regional regulation of microtubule dynamics in motile fibroblasts. *Cell.* 104:923–935.

Berrueta, L., J.S. Tirnauer, S.C. Schuyler, D. Pellman, and B.E. Bierer. 1999. The APC-associated protein EB1 associates with components of the dynactin complex and cytoplasmic dynein intermediate chain. *Curr. Biol.* 9:425–428.

Burkhardt, J.K., C.J. Echeverri, T. Nilsson, and R.B. Vallee. 1997. Overexpression of the dynamitin (p50) subunit of the dynactin complex disrupts dynein-dependent maintenance of membrane organelle distribution. *J. Cell Biol.* 139:469–484.

Carminati, J.L., and T. Stearns. 1997. Microtubules orient the mitotic spindle in yeast through dynein-dependent interactions with the cell cortex. *J. Cell Biol.* 138:629–641.

Coquelle, F.M., M. Caspi, F.P. Cordelieres, J.P. Dompierre, D.L. Dujardin, C. Koifman, P. Martin, C.C. Hoogenraad, A. Akhmanova, N. Galjart, et al. 2002. LIS1, CLIP-170's key to the dynein/dynactin pathway. *Mol. Cell. Biol.* 22:3089–3102.

Corthesy-Theulaz, I., A. Pauloin, and S.R. Pfeffer. 1992. Cytoplasmic dynein participates in the centrosomal localization of the Golgi complex. *J. Cell Biol.* 118:1333–1345.

Desai, A., and T.J. Mitchison. 1997. Microtubule polymerization dynamics. *Annu. Rev. Cell Dev. Biol.* 13:83–117.

Dhamodharan, R., and P. Wadsworth. 1995. Modulation of microtubule dynamic instability in vivo by brain microtubule associated proteins. *J. Cell Sci.* 108:1679–1689.

Dujardin, D., U.I. Wacker, A. Moreau, T.A. Schroer, J.E. Rickard, and J.R. De Mey. 1998. Evidence for a role of CLIP-170 in the establishment of metaphase chromosome alignment. *J. Cell Biol.* 141:849–862.

Farshori, P., and E.L. Holzbaur. 1997. Dynactin phosphorylation is modulated in response to cellular effectors. *Biochem. Biophys. Res. Commun.* 232:810–816.

Faulkner, N.E., D.L. Dujardin, C.Y. Tai, K.T. Vaughan, C.B. O'Connell, Y. Wang, and R.B. Vallee. 2000. A role for the lissencephaly gene LIS1 in mitosis and cytoplasmic dynein function. *Nat. Cell Biol.* 2:784–791.

Garces, J.A., I.B. Clark, D.I. Meyer, and R.B. Vallee. 1999. Interaction of the p62 subunit of dynactin with Arp1 and the cortical actin cytoskeleton. *Curr. Biol.* 9:1497–1500.

Gill, S.R., T.A. Schroer, I. Szilak, E.R. Steuer, M.P. Sheetz, and D.W. Cleveland. 1991. Dynactin, a conserved, ubiquitously expressed component of an activator of vesicle motility mediated by cytoplasmic dynein. *J. Cell Biol.* 115:1639–1650.

Habermann, A., T.A. Schroer, G. Griffiths, and J.K. Burkhardt. 2001. Immunolocalization of cytoplasmic dynein and dynactin subunits in cultured macrophages: enrichment on early endocytic organelles. *J. Cell Sci.* 114:229–240.

Hayden, J.H., S.S. Bowser, and C.L. Rieder. 1990. Kinetochores capture astral microtubules during chromosome attachment to the mitotic spindle: direct visualization in live newt lung cells. *J. Cell Biol.* 111:1039–1045.

Holleran, E.A., M.K. Tokito, S. Karki, and E.L. Holzbaur. 1996. Centractin (ARP1) associates with spectrin revealing a potential mechanism to link dynactin to intracellular organelles. *J. Cell Biol.* 135:1815–1829.

Holzbaur, E.L.F., J.A. Hammarback, B.M. Paschal, N.G. Kravit, K.K. Pfister, and R.B. Vallee. 1991. Homology of a 150 kD cytoplasmic dynein-associated polypeptide with the *Drosophila* gene glued. *Nature.* 351:579–583.

Hoogenraad, C.C., A. Akhmanova, F. Grosveld, C.I. De Zeeuw, and N. Galjart. 2000. Functional analysis of CLIP-115 and its binding to microtubules. *J. Cell Sci.* 113:2285–2297.

Huitorel, P., and M.W. Kirschner. 1988. The polarity and stability of microtubule capture by the kinetochore. *J. Cell Biol.* 106:151–159.

Karki, S., and E.L. Holzbaur. 1995. Affinity chromatography demonstrates a direct binding between cytoplasmic dynein and the dynactin complex. *J. Biol. Chem.* 270:28806–28811.

King, S.J., and T.A. Schroer. 2000. Dynactin increases the processivity of the cytoplasmic dynein motor. *Nat. Cell Biol.* 2:20–24.

Lippincott-Schwartz, J., J.G. Donaldson, A. Schweizer, E.G. Berger, H.-P. Hauri, L.C. Yuan, and R.D. Klausner. 1990. Microtubule-dependent retrograde transport of proteins in the ER in the presence of brefeldin A suggests an ER recycling pathway. *Cell.* 60:821–836.

Mimori-Kiyosue, Y., N. Shiina, and S. Tsukita. 2000a. Adenomatous polyposis coli (APC) protein moves along microtubules and concentrates at their growing ends in epithelial cells. *J. Cell Biol.* 148:505–518.

Mimori-Kiyosue, Y., N. Shiina, and S. Tsukita. 2000b. The dynamic behavior of the APC-binding protein EB1 on the distal ends of microtubules. *Curr. Biol.* 10:865–868.

Mitchison, T.J., and M.W. Kirschner. 1985. Properties of the kinetochore in vitro. II. Microtubule capture and ATP- dependent translocation. *J. Cell Biol.* 101:766–777.

Morrison, E.E., B.N. Wardleworth, J.M. Askham, A.F. Markham, and D.M. Meredith. 1998. EB1, a protein which interacts with the APC tumour suppressor, is associated with the microtubule cytoskeleton throughout the cell cycle. *Oncogene.* 17:3471–3477.

Nathke, I.S., C.L. Adams, P. Polakis, J.H. Sellin, and W.J. Nelson. 1996. The adenomatous polyposis coli tumor suppressor protein localizes to plasma membrane sites involved in active cell migration. *J. Cell Biol.* 134:165–179.

Paschal, B.M., E.L. Holzbaur, K.K. Pfister, S. Clark, D.I. Meyer, and R.B. Vallee. 1993. Characterization of a 50-kDa polypeptide in cytoplasmic dynein preparations reveals a complex with p150GLUED and a novel actin. *J. Biol. Chem.* 268:15318–15323.

Perez, F., G.S. Diamantopoulos, R. Stalder, and T.E. Kreis. 1999. CLIP-170 highlights growing microtubule ends *in vivo*. *Cell.* 96:517–527.

Pierre, P., J. Scheel, J.E. Rickard, and T.E. Kreis. 1992. CLIP-170 links endocytic vesicles to microtubules. *Cell.* 70:887–900.

Presley, J.F., N.B. Cole, T.A. Schroer, K. Hirschberg, K.J. Zaal, and J. Lippincott-Schwartz. 1997. ER-to-Golgi transport visualized in living cells. *Nature.* 389:81–85.

Reese, E.L., and L.T. Haimo. 2000. Dynein, dynactin, and kinesin II's interaction with microtubules is regulated during bidirectional organelle transport. *J. Cell Biol.* 151:155–166.

Rickard, J.E., and T.E. Kreis. 1991. Binding of pp170 to microtubules is regulated by phosphorylation. *J. of Biol. Chem.* 266:17597–17605.

Sammak, P.J., and G.G. Borisy. 1988. Direct observation of microtubule dynamics in living cells. *Nature.* 332:724–726.

Schroer, T.A., and M.P. Sheetz. 1991. Two activators of microtubule-based vesicle transport. *J. Cell Biol.* 115:1309–1318.

Schuyler, S.C., and D. Pellman. 2001. Search, capture and signal: games microtubules and centrosomes play. *J. Cell Sci.* 114:247–255.

Shima, D.T., K. Haldar, R. Pepperkok, R. Watson, and G. Warren. 1997. Partitioning of the Golgi apparatus during mitosis in living HeLa cells. *J. Cell Biol.* 137:1211–1228.

Tai, C.Y., D.L. Dujardin, N.E. Faulkner, and R.B. Vallee. 2002. Role of dynein, dynactin, and CLIP-170 interactions in LIS1 kinetochore function. *J. Cell Biol.* 156:959–968.

Valetti, C., D.M. Wetzel, M. Schrader, M.J. Hasbani, S.R. Gill, T.E. Kreis, and T.A. Schroer. 1999. Role of dynactin in endocytic traffic: effects of dynamitin overexpression and colocalization with CLIP-170. *Mol. Biol. Cell.* 10:4107–4120.

Vaughan, K.T., and R.B. Vallee. 1995. Cytoplasmic dynein binds dynactin through a direct interaction between the intermediate chains and p150*Glued*. *J. Cell Biol.* 131:1507–1516.

Vaughan, K.T., S.H. Hughes, C.J. Echeverri, N.F. Faulkner, and R.B. Vallee. 1999. Co-localization of dynactin and cytoplasmic dynein with CLIP-170 at microtubules distal ends. *J. Cell Sci.* 112:1437–1447.

Vaughan, P.S., J.D. Leszyk, and K.T. Vaughan. 2001. Cytoplasmic dynein intermediate chain phosphorylation regulates binding to dynactin. *J. Biol. Chem.* 276:26171–26179.

Waterman-Storer, C.M., S. Karki, and E.L. Holzbaur. 1995. The p150Glued component of the dynactin complex binds to both microtubules and the actin-related protein centractin (Arp-1). *Proc. Natl. Acad. Sci. USA.* 92:1634–1638.

Waterman-Storer, C.M., A. Desai, J.C. Bulinski, and E.D. Salmon. 1998. Fluorescent speckle microscopy, a method to visualize the dynamics of protein assemblies in living cells. *Curr. Biol.* 8:1227–1230.

Xiang, X., G. Han, D.A. Winkelmann, W. Zuo, and N.R. Morris. 2000. Dynamics of cytoplasmic dynein in living cells and the effect of a mutation in the dynactin complex actin-related protein Arp1. *Curr. Biol.* 10:603–606.